

Analysis of Coherent Heteroclustering of Different Dyes by Use of Threoninol Nucleotides for Comparison with the Molecular Exciton Theory

Taiga Fujii,^[a] Hiromu Kashida,^[a] and Hiroyuki Asanuma*^[a, b]

Abstract: To test the molecular exciton theory for heterodimeric chromophores, various heterodimers and clusters, in which two different dyes were stacked alternately, were prepared by hybridizing two oligodeoxyribonucleotides (ODNs), each of which tethered a different dye on D-threoninol at the center of the strand. NMR analyses revealed that two different dyes from each strand were stacked antiparallel to each other in the duplex, and were located adjacent to the 5'-side of a natural nucleobase. The spectroscopic behavior of these heterodimers was systematically examined as a function of the difference in the wavelength of the dye absorption maxima ($\Delta\lambda_{\max}$). We found that the absorption spectrum of the heterodimer was significantly different from that of the simple sum of each monomeric dye in the single

strand. When azobenzene and Methyl Red, which have λ_{\max} at 336 and 480 nm, respectively, in the single strand ($\Delta\lambda_{\max}=144$ nm), were assembled on ODNs, the band derived from azobenzene exhibited a small hyperchromism, whereas the band from Methyl Red showed hypochromism and both bands shifted to a longer wavelength (bathochromism). These hyper- and hypochromisms were further enhanced in a heterodimer derived from 4'-methylthioazobenzene and Methyl Red, which had a much smaller $\Delta\lambda_{\max}$ (82 nm; $\lambda_{\max}=398$ and 480 nm in the single-strand, respectively). With a combination of 4'-dimethyl-

amino-2-nitroazobenzene and Methyl Red, which had an even smaller $\Delta\lambda_{\max}$ (33 nm), a single sharp absorption band that was apparently different from the sum of the single-stranded spectra was observed. These changes in the intensity of the absorption band could be explained by the molecular exciton theory, which has been mainly applied to the spectral behavior of H- and/or J-aggregates composed of homo dyes. However, the bathochromic band shifts observed at shorter wavelengths did not agree with the hypochromism predicted by the theory. Thus, these data experimentally verify the molecular exciton theory of heterodimerization. This coherent coupling among the heterodimers could also partly explain the bathochromicity and hypochromicity that were observed when the dyes were intercalated into the duplex.

Keywords: DNA • exciton theory • heteroclusters • NMR spectroscopy • UV/Vis spectroscopy

Introduction

Assembly of a dye induces characteristic spectroscopic behavior, such as band narrowing and band shifts, that cannot be achieved with a monomeric dye.^[1] Furthermore, since

dye assemblies have the potential to contribute to the production of nonlinear optical materials^[2] and light-harvesting systems,^[3] the preparation of ordered dye assemblies and their characterization is very important both from a scientific and a practical point of view. To date, various methodologies for the preparation of homo-assemblies composed of identical dyes have been proposed, and their spectroscopic behaviors, such as J- and H-bands, have been examined theoretically on the basis of molecular exciton theory.^[1,4] However, due to the difficulty of their preparation, there have only been a limited number of reports on the characterization of hetero-assemblies, especially those of a predetermined size and orientation.^[5-7] Hence, theoretical investigation of the spectroscopic behavior and potential applications of hetero-assemblies is less advanced than that of homo-assemblies, at least in part because theoretical calculations concerning their spectroscopic behavior cannot be experi-

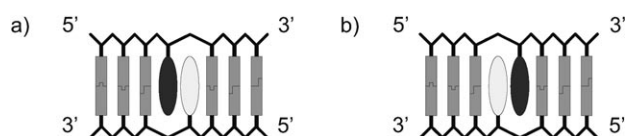
[a] T. Fujii, Dr. H. Kashida, Prof. Dr. H. Asanuma
Department of Molecular Design and Engineering
Graduate School of Engineering, Nagoya University
Furo-cho, Chikusa-ku, Nagoya 464-8603 (Japan)
Fax: (+81)52-789-2528
E-mail: asanuma@mol.nagoya-u.ac.jp

[b] Prof. Dr. H. Asanuma
Core Research for Evolution Science and Technology (CREST)
Japan Science and Technology Agency (JST)
Kawaguchi, Saitama 332-0012 (Japan)

Supporting information for this article is available on the WWW under <http://dx.doi.org/10.1002/chem.200900962>.

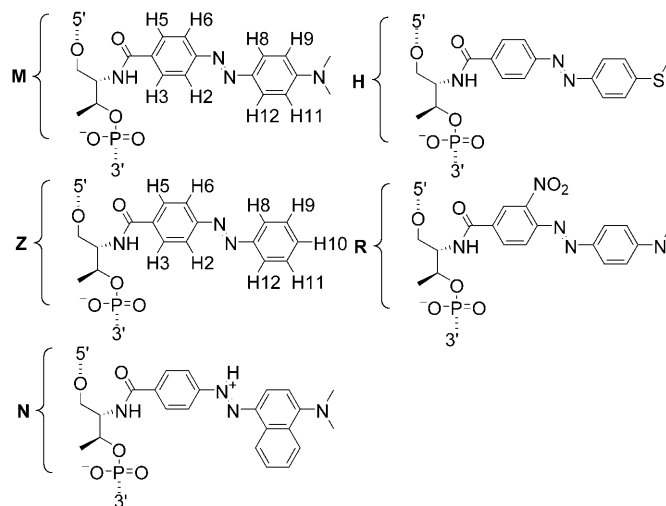
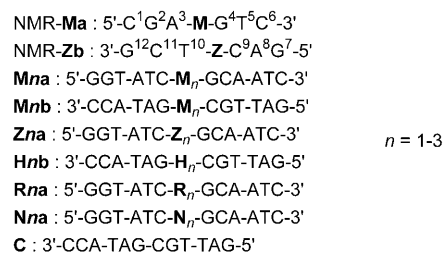
mentally verified. As far as we know, there are only a few examples that demonstrate a relationship between the experimental observation of the spectroscopic behavior of heteroaggregation (dimerization) and its theoretical prediction. The first report of this type was by Kuhn et al. on the spectroscopic behavior of a heterodimer of cyanine dyes spread on the water/air interface using the Langmuir–Blodgett method.^[6] Furthermore, a change in the absorption spectra of a fluorescence resonance energy transfer (FRET) donor–acceptor pair and/or an fluorescein isothiocyanate/dimethyl aminophenylazo benzoic acid (FITC/Dabcyl; Methyl Red) pair tethered at both the 3'- and 5'-termini of a molecular beacon has been demonstrated.^[7,8] However, since mutual orientation of these heterodimers was not well-defined and was difficult to control, they were not appropriate models to verify the exciton theory experimentally. Furthermore, these investigations lacked the viewpoint of the difference of λ_{\max} , which should significantly affect the coherency of the dimers. Verification of the exciton theory will lead to the design of new hetero-assemblies having special optical properties that cannot be realized by homo-assemblies.

Previously, we proposed a unique method for the preparation of a dye assembly by hybridization of two single-stranded oligodeoxyribonucleotides (ODNs), each of which tethered dyes to D-threoninols (threoninol nucleotides) at the center of the strand.^[9] The use of threoninol as a dye scaffold allows easy programming of various dye assemblies that are difficult to design based on the conventional self-association of dyes. Alternating heteroclusters of a predetermined size and orientation can be easily prepared by hybridization of two complementary DNA–dye conjugates, each of which is conjugated to a different dye. In the present study, we prepared various heterodimers of Methyl Red with other dyes using threoninol nucleotides. The dyes chosen for heterodimerization with Methyl Red were chosen with a focus on the difference in λ_{\max} between Methyl Red and the second dye ($\Delta\lambda_{\max}$), as shown in Schemes 1 and 2. Such a



Scheme 1. Schematic illustration of the design of the heterodimer using threoninol nucleotides as dye tethers. There are two possible dye locations: the dyes are located adjacent to a) the 5'-side (corresponding to **M/Z** orientation in NMR-**Ma**/NMR-**Zb**) or b) the 3'-side of a natural nucleobase (corresponding to **Z/M** orientation).

systematic investigation of the relationship between $\Delta\lambda_{\max}$ and coherency in a firmly stacked heterodimer of predetermined orientation has not yet been reported. The stacked structure of the heterodimer in the duplex was first determined by NMR analysis,^[10] and the spectroscopic behavior of the dyes was then investigated in detail in order to verify qualitatively the predictions of the molecular exciton theory. We used azo compounds as model dyes because: 1) the mo-



Scheme 2. Sequence of the ODNs synthesized in this study.

lecular sizes of these dyes are very similar; 2) the π – π^* transition (light absorption) of these dyes occurs in a similar manner; 3) they have a single and fairly symmetrical absorption band; and 4) the absorption spectra reflect the exciton coupling (coherency) of the dyes rather than fluorescence. Five threoninol nucleotides with azobenzene (**Z**), 4'-methylthioazobenzene (**H**), Methyl Red (**M**), 4'-dimethylamino-2-nitroazobenzene (**R**), or Naphthyl Red (**N**) tethers were incorporated into ODNs (see Scheme 2 for the structures), and various heterodimers were prepared to investigate their spectroscopic behavior from both experimental and theoretical viewpoints. These insights into heterodimerization will lead to the design of more sensitive fluorophore–quencher pairs of molecular beacons.

Results

Structural determination of the heterodimers by NMR spectroscopy: As illustrated in Scheme 1, heterodimer formation is based on the tentative base-pairing of threoninol nucleotides at the center of paired ODNs. A dye residue is located at the counterpart of the other dye residue in the complementary ODN sequence,^[11] and these dye residues from the two strands stack with each other, in an antiparallel orientation, by pseudo “base-pairing”. The ODNs synthesized for this study are outlined in Scheme 2. We first conducted an NMR analysis of a heteroduplex of ODNs conjugated with Methyl Red and azobenzene (NMR-**Ma**/NMR-**Zb**, respec-

tively), in order to determine the location of the stacked **M** and **Z** in the duplex. There are two possible locations of the dyes: adjacent to the 5'-side (Scheme 1 a, **M/Z**) or to the 3'-side (Scheme 1 b, **Z/M**) of the natural nucleobase.

Because the melting temperature of the NMR-**Ma**/NMR-**Zb** duplex was determined to be 22.1 °C,^[12] NMR measurements were performed at 5 °C (278 K), a temperature at which a stable duplex exists. In order to monitor imino protons, which are exchangeable with water molecules, NMR was measured in H₂O (H₂O/D₂O, 9:1) with a 3-9-19 WATERGATE pulse sequence for H₂O suppression.^[13] When these data were combined with the NOESY, DQF-COSY, and TOCSY spectra obtained in H₂O, most of the signals of the duplex could be assigned. The one-dimensional NMR spectrum measured in H₂O at the region of imino protons (11–14 ppm) is depicted in Figure 1. The NMR-**Ma**/

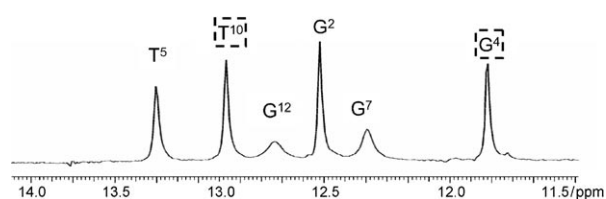


Figure 1. 1D NMR spectrum of the NMR-**Ma**/NMR-**Zb** duplex at the imino region in H₂O/D₂O 9:1 at 278 K (mixing time = 150 ms), pH 7.0 (20 mM phosphate buffer), in the presence of 200 mM NaCl. The concentration of NMR-**Ma**/NMR-**Zb** was 1.0 mM. Assignments of the imino-protons and the residue number are denoted at the top of the peak.

NMR-**Zb** duplex allowed six natural base-pairs (C¹-G¹², G²-C¹¹, A³-T¹⁰, G⁴-C⁹, T⁵-A⁸, and C⁶-G⁷), and one tentative **M-Z** pair (Scheme 2). As expected, there were six individual signals that could be assigned on the basis of the NOESY and chemical shift of each signal, indicating that the non-natural **M** and **Z** did not interrupt the base-pairing. The imino proton signals of the terminal G⁷ and G¹² were rather broad, because of the rapid exchange with water, whereas signals from the other residues remained sharp. Figure 2 depicts the NOEs between the imino proton signal (11–14 ppm) and the aromatic proton signal (5.5–7.5 ppm) regions. A distinct NOE signal was observed between the imino proton of T¹⁰ and H8 (H12) of the Methyl Red protons, indicating that the Methyl Red moiety was located at around T¹⁰. In addition, strong NOE signals were detected between the imino proton of G⁴ and H2 (H6) and H8 (H12) of the azobenzene protons, indicating that the azobenzene moiety was located in the vicinity of G⁴. Thus, we could unambiguously conclude that each dye was located adjacent to the 5'-side of the natural nucleobase (**M/Z**, corresponding to Scheme 1 a).

Evidence for antiparallel stacking of **M** and **Z** was given by the NOESY spectrum between the regions of 5.5–7.5 ppm and 1.0–2.6 ppm (Figure 3). Strong NOE signals were observed between N-CH₃ of **M** and H2 (H6) of **Z**, as well as between N-CH₃ of **M** and H3 (H5) of **Z**, indicating that **M** and **Z** were stacked in an antiparallel manner. The

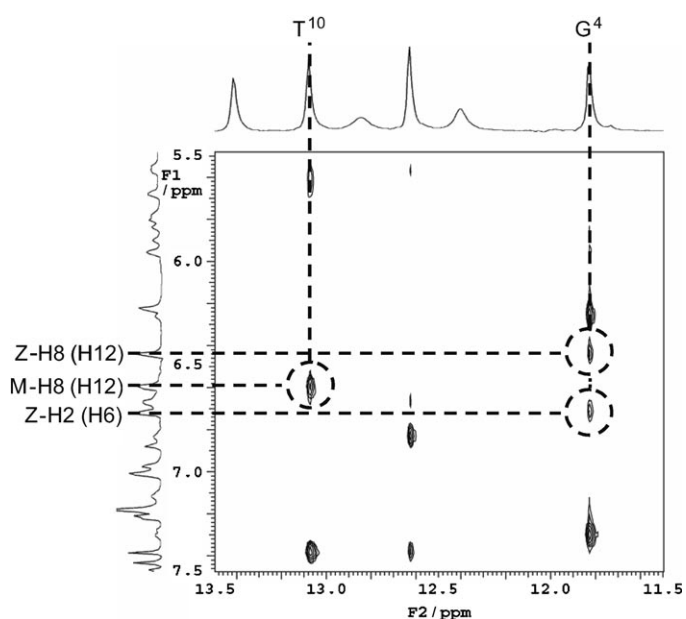


Figure 2. 2D NOESY spectrum (mixing time = 150 ms) between the imino-proton signal (11–14 ppm) and the aromatic-proton signal regions (5.5–7.5 ppm) for the NMR-**Ma**/NMR-**Zb** duplex in H₂O/D₂O 9:1 at 278 K, pH 7.0 (20 mM phosphate buffer), in the presence of 200 mM NaCl. Assignments of the Methyl Red and azobenzene protons are denoted on the 1D spectra (F1 axis) with the numbers designated in Scheme 2. The NOE signals surrounded by broken circles demonstrate intercalation of the Methyl Red and azobenzene.

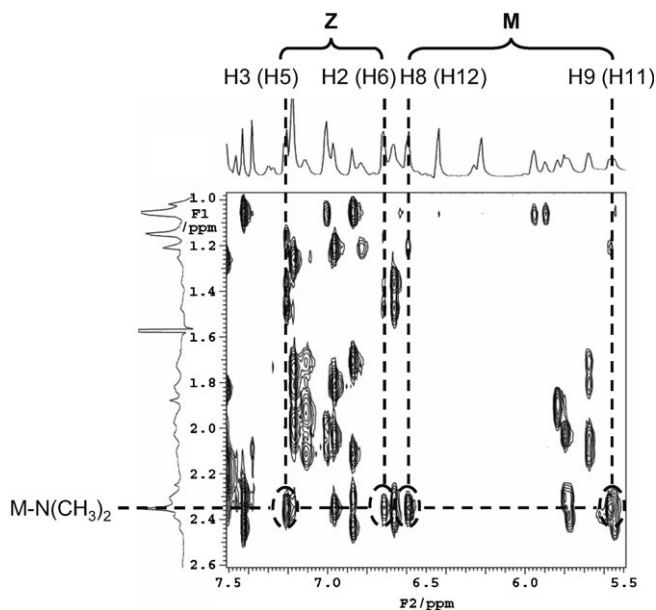


Figure 3. 2D NOESY spectrum (mixing time = 150 ms) between the regions of 5.5–7.5 ppm and 1.0–2.6 ppm for the NMR-**Ma**/NMR-**Zb** duplex in H₂O/D₂O 9:1 at 278 K (20 mM phosphate buffer), in the presence of 200 mM NaCl.

combined NOE signals demonstrate that **M** and **Z** are stacked antiparallel to each other and are located adjacent to the 5'-side of the nucleobase, as depicted in Figure 4 a,

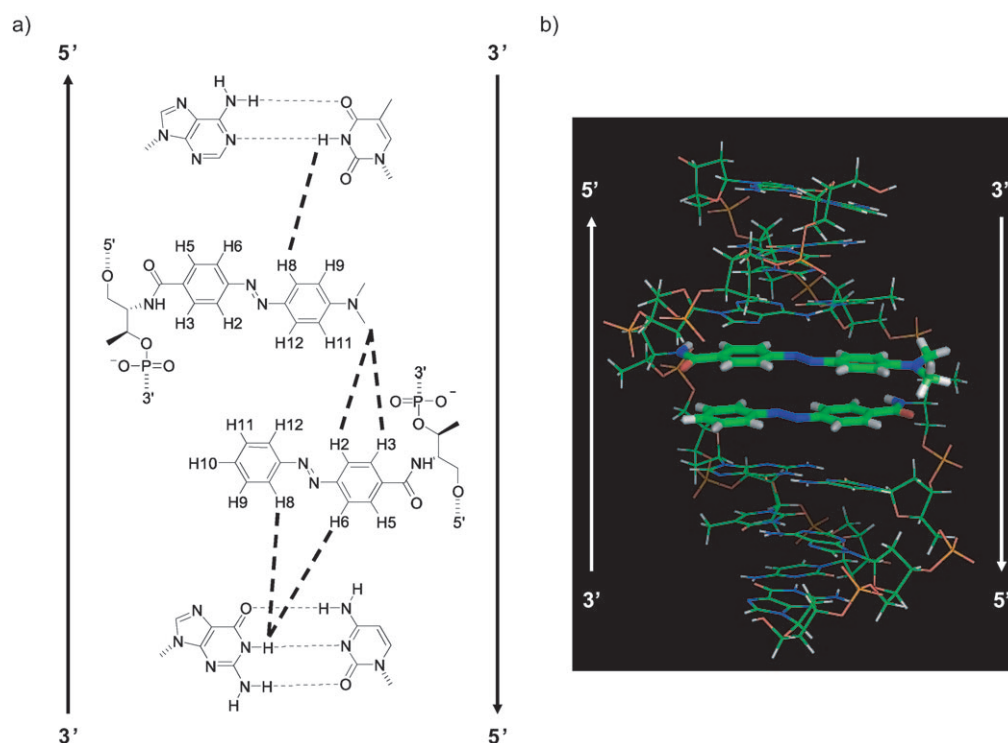


Figure 4. a) Stacking manner and orientation of **Z** and **M** residues in the duplex determined from NOESY, and b) an energy-minimized structure of the NMR-**Ma**/NMR-**Zb** duplex calculated with InsightII/Discover3 from the initial structure determined by NMR analyses. Broken lines in a) show the observed NOE signals. The sticks in b) depict azobenzene and Methyl Red in the duplex.

which validates our design of the heterodimer. Computer modeling of NMR-**Ma**/NMR-**Zb**, using the InsightII/discover3 software, was entirely consistent with the NMR analyses (Figure 4b).

Spectroscopic behavior of the alternate heterodimers:

Having validated our heterodimer design and confirmed its stacked structure, we next investigated spectral changes of heterodimers composed of the various ODN–dye conjugates shown in Scheme 2. This analysis focused on the difference of λ_{\max} between the dyes ($\Delta\lambda_{\max}$) in the heterodimer.

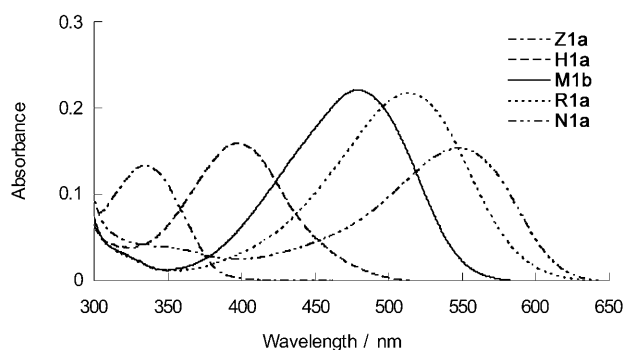


Figure 5. UV/Vis spectra of single-stranded **Z1a**, **H1a**, **N1a**, **R1a**, and **M1b** at 0°C that corresponded to a monomeric transition. Solution conditions were as follows: [ODN]=5 μM , [NaCl]=100 mM, pH 7.0 (10 mM phosphate buffer). For the measurement of **N1a**, 10 mM MES buffer at pH 5.0 was used.

Figure 5 shows the UV/Vis spectra of the single-stranded dye conjugates synthesized in this study. These conjugates, **Z1a**, **H1a**, **M1b**, **R1a**, and **N1a**, showed absorption maxima at 336, 398, 480, 513, and 548 nm, respectively. The absorption maxima corresponded to a monomeric transition at 0°C, which is controlled by the introduction of electron-donating and electron-attracting functional groups to the azobenzene scaffold.^[14] We then prepared four different kinds of heteroclusters by combining Methyl Red-conjugated ODNs (**Mnb**) with ODNs conjugated with the other dyes, thus forming **Zna/Mnb**, **Hna/Mnb**, **Rna/Mnb**, and **Nna/Mnb** heterodimers. A summary of the λ_{\max} of the single conjugates and the $\Delta\lambda_{\max}$ between **M1b** and the other dye conjugates is shown in Table 1.

Table 1. Absorption maxima (λ_{\max}) of single-stranded dye-conjugates corresponding to a monomeric transition, and the $\Delta\lambda_{\max}$ between **M1b** and the conjugates used in this study.

| Sequences | λ_{\max} [nm] (ν_{\max} [cm^{-1}]) ^[a] | $\Delta\lambda_{\max}$ [nm] ($\Delta\nu_{\max}$ [cm^{-1}]) ^[a] |
|------------|---|---|
| M1b | 480 (2.08×10^4) | – |
| Z1a | 336 (2.98×10^4) | 144 (8.93×10^3) |
| H1a | 398 (2.51×10^4) | 82 (4.29×10^3) |
| R1a | 513 (1.95×10^4) | 33 (1.34×10^3) |
| N1a | 548 (1.82×10^4) ^[b] | 68 (2.59×10^3) ^[b] |

[a] Measurement conditions were pH 7.0 (10 mM phosphate buffer), [ODN]=5 μM , [NaCl]=100 mM, at 0°C. [b] Measurement conditions were pH 5.0 (10 mM MES buffer), [ODN]=5 μM , [NaCl]=100 mM, at 0°C.

Z/M combination ($\Delta\lambda_{\max}=144$ nm): Figure 6 shows the UV/Vis spectra of **Z1a/M1b**, **Z1a**, **M1b**, and a spectrum calculated as the simple sum of the two single strands (sum-spec-

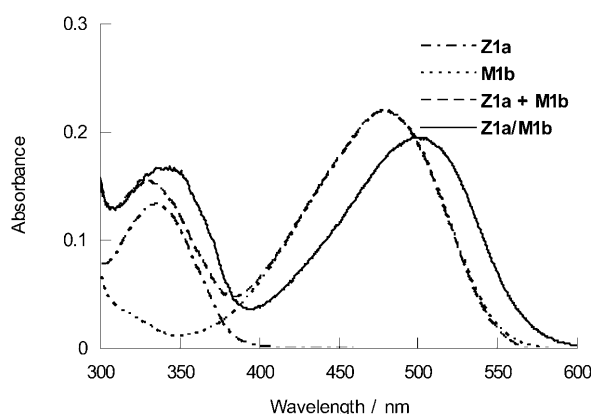


Figure 6. UV/Vis spectra of the **Z1a/M1b** duplex (solid line), single-stranded **Z1a** (dashed-dotted line), **M1b** (dotted line), and a simple sum of their spectra (sum-spectrum, **Z1a + M1b**, dashed line) at 0°C. Solution conditions were as follows: [ODN]=5 μ M, [NaCl]=100 mM, pH 7.0 (10 mM phosphate buffer).

trum). Both single-stranded **Z1a** and **M1b** exhibited broad bands (peaks) at 336 and 480 nm, respectively. The sum-spectrum gave two bands because $\Delta\lambda_{\max}$ of **Z1a/M1b** was as high as 144 nm. The absorption spectrum of the **Z1a/M1b** duplex also gave two bands at around 344 and 500 nm, although the pattern was slightly but distinctly different from the pattern for the sum of each spectrum. Dimerization of **Z** and **M** induced a bathochromic shift in the λ_{\max} of both dyes. In addition, the peak located at a shorter wavelength in **Z1a/M1b** (derived from the single-stranded **Z**) showed hyperchromism. In contrast, hypochromism was observed for the peak derived from the single-stranded **M**.

H/M combination ($\Delta\lambda_{\max}=82$ nm): An **H/M** combination of the dyes gave a $\Delta\lambda_{\max}$ of 82 nm, which was half that of the **Z1a** and **M1b** combination. The absorption spectra of **H1a/M1b**, **H1a**, **M1b**, and their sum-spectrum are depicted in Figure 7a. Interestingly, hybridization of these two conjugates displayed an absorption spectrum that was apparently different from that of the sum of their single strands. The UV/Vis spectrum of the **H1a/M1b** duplex gave one main band at 422 nm and a shoulder band at around 480–560 nm, as depicted by the solid line in Figure 7a, whereas the sum-spectrum of **H1a** and **M1b** (dashed line in Figure 7a) showed two broad bands with almost equal absorbance at 398 and 480 nm. Following hybridization, the absorption band at 398 nm, corresponding to **H1a**, showed both strong bathochromicity and hyperchromicity, whereas the band at 480 nm, corresponding to **M1b**, displayed bathochromicity and hypochromicity (Figure 7a). Although this tendency was similar to that observed with the **Z1a** and **M1b** combination, the spectral change induced by hybridization was

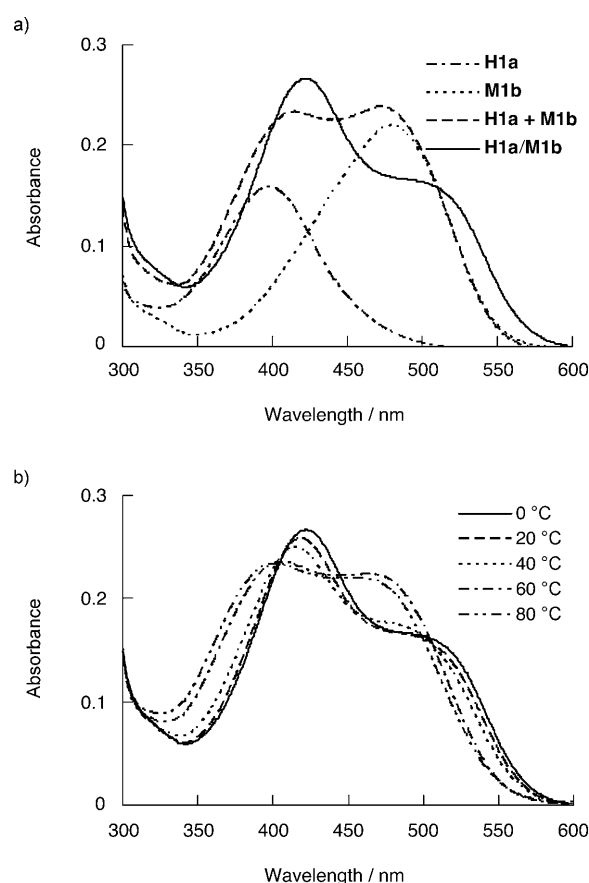


Figure 7. a) UV/Vis spectra of **H1a/M1b** duplex (solid line), single-stranded **H1a** (dashed-dotted line), **M1b** (dotted line), and a simple sum of their spectra (sum-spectrum, **H1a + M1b**, dashed line) at 0°C, and b) the effect of temperature on the absorption spectrum of **H1a/M1b**. Solution conditions were as follows: [ODN]=5 μ M, [NaCl]=100 mM, pH 7.0 (10 mM phosphate buffer).

further amplified with the **H1a** and **M1b** combination, which had a smaller $\Delta\lambda_{\max}$. In order to rule out the possibility that these spectral behaviors were due to an unexpected covalent interaction of these dyes, thermal reversibility of the **H1a/M1b** duplex was examined. The absorption spectrum of **H1a/M1b** above 60°C, a temperature at which the duplex was completely dissociated, was similar to the sum-spectrum of **H1a** and **M1b** (compare the dashed line in Figure 7a with the dashed-dotted line in Figure 7b). Note that the melting temperature (T_m) of **H1a/M1b** was 51.2°C under the conditions employed (see Supporting Information, Table 1). In contrast, a reduction in temperature below T_m allowed a large, reversible, spectroscopic change. Thus, the spectral changes observed in the duplex were confirmed to be due to a noncovalent interaction between **H** and **M** in the duplex. Since further reduction in temperature from 40 to 0°C slightly changed their absorption spectra, chromophore motions would also affect the exciton interaction slightly.^[15]

R/M and N/M combination ($\Delta\lambda_{\max}=33$ and 68 nm): The combination of **R** and **M** had the smallest $\Delta\lambda_{\max}$ (33 nm) of

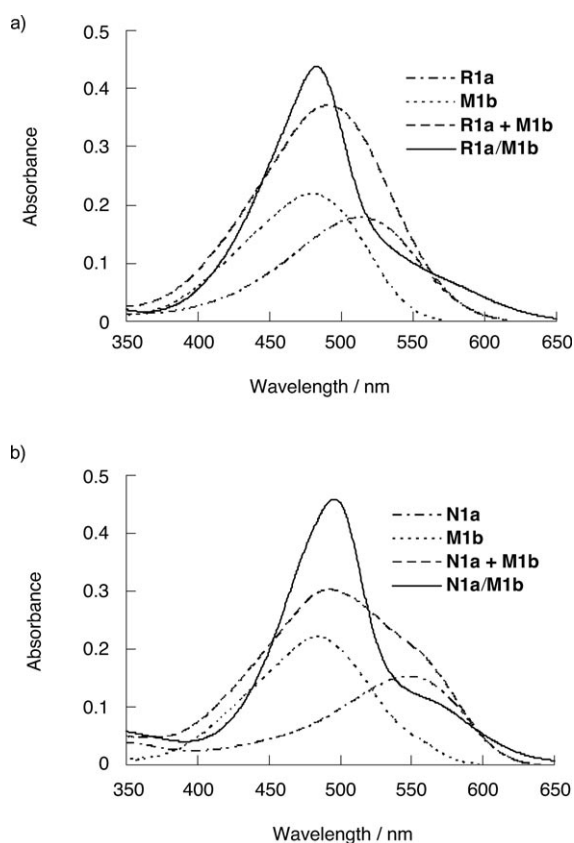


Figure 8. a) UV/Vis spectra of the **R1a/M1b** duplex (solid line), single-stranded **R1a** (dashed-dotted line), **M1b** (dotted line), and a simple sum of their spectra (sum-spectrum, **R1a + M1b**, dashed line) at 0°C. Solution conditions were as follows: [ODN]=5 μ M, [NaCl]=100 mM, pH 7.0 (10 mM phosphate buffer). b) UV/Vis spectra of the **N1a/M1b** duplex (solid line), single-stranded **N1a** (dashed-dotted line), **M1b** (dotted line), and a simple sum of their spectra (sum-spectrum, **N1a + M1b**, dashed line) at 0°C. Solution conditions were as follows: [ODN]=5 μ M, [NaCl]=100 mM, pH 5.0 (10 mM MES buffer).

all the combinations examined in this study. Hence, the sum-spectrum of these two single strands gave not two, but one broad single band, due to the proximity of the absorption maxima. When these two conjugates were hybridized, however, a single sharp absorption band appeared at 483 nm, with a broad, weak shoulder at 550–650 nm, which was entirely different from the pattern of the sum-spectrum, as shown in Figure 8a. Similarly, **N1a/M1b**, which we previously demonstrated as an alternating heterocluster,^[9] also showed a single absorption band at 496 nm with a broad weak shoulder (Figure 8b).

Effect of aggregate size on spectroscopic behavior of alternating heteroclusters: We next examined the effect of alternating heteroclustering of **Hna/Mnb** and **Rna/Mnb**, both of which exhibited a large spectral change upon dimerization. As shown in Figure 9a, an increase in dye number in **Hna/Mnb** ($n=1-3$) increased the absorbance of the band of shorter wavelength, whereas little increase was observed in

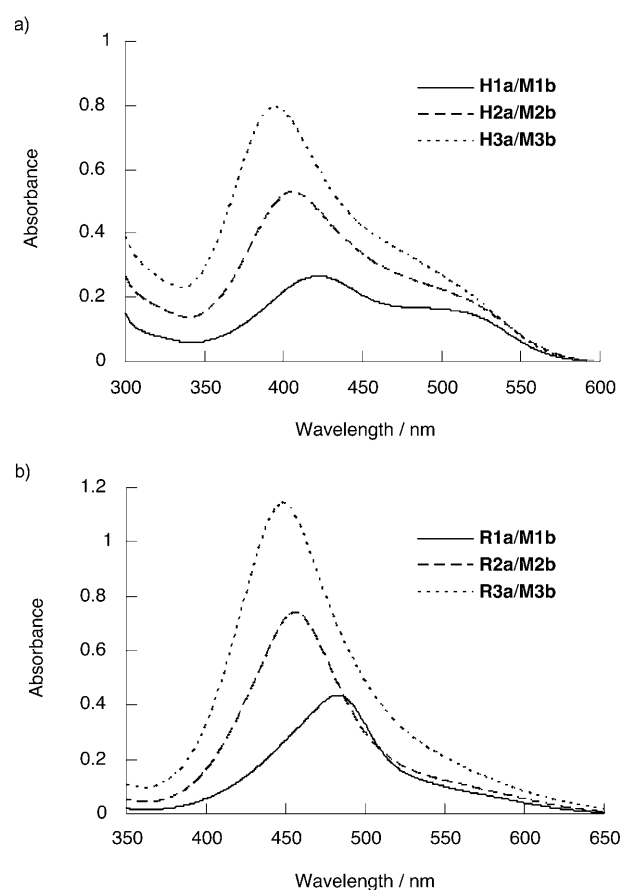


Figure 9. Effect of the number of dye pairs on the UV/Vis spectra of a) **Hna/Mnb**, and b) **Rna/Mnb** combinations. Solution conditions were as follows: 0°C, [ODN]=5 μ M, [NaCl]=100 mM, pH 7.0 (10 mM phosphate buffer).

the shoulder band of the longer wavelength. Consequently, **H3a/M3b** exhibited almost a single band with a broad shoulder. In addition, prominent hypsochromism was induced as the size of the aggregates increased. In the case of **Rna/Mna**, the single sharp band that appeared at 483 nm in **R1a/M1b** grew as the number of dyes incorporated per strand increased ($n=1-3$) and was accompanied by a distinct hypsochromic shift, as depicted in Figure 9b. The spectroscopic behavior of these ODNs with higher numbers of dyes incorporated was similar to that of homo H-aggregates, which exhibit hypsochromic shifts and sharp bands.^[16] **N/M** pairs with a $\Delta\lambda_{\max}$ of 68 nm also showed a similar spectroscopic behavior to **R/M** pairs with an increase in the cluster size (see Figure 1 in Supporting Information).

The effect of cluster size on circular dichroism (CD) spectra is shown in Figure 10. Although heteroclusters were stably formed below T_m for both **Hna/Mnb** and **Rna/Mnb**, the induced CD (ICD) at the $\pi-\pi^*$ transition region was not so strong. A small ICD is interpreted as an unwound structure of a stacked dye assembly on D-threosinol. In a Methyl Red homocluster, this would result in a ladder-like structure due to its flexibility, as previously demonstrated.^[9b]

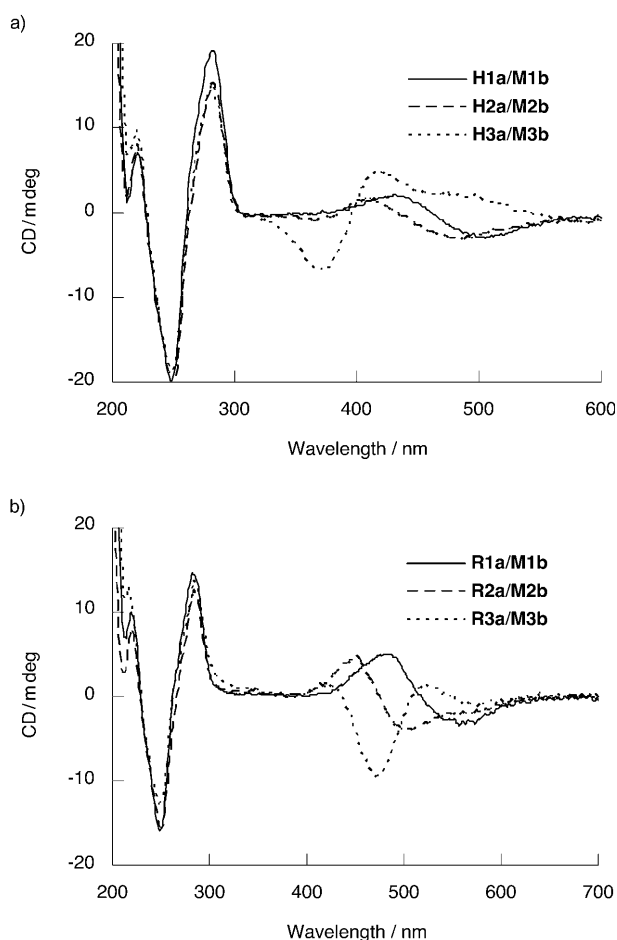


Figure 10. Effect of the number of dye pairs on the CD spectra of a) **Hna/Mnb**, and b) **Rna/Mnb** combinations. Solution conditions were as follows: 0 °C, [ODN] = 5 μ M, [NaCl] = 100 mM, pH 7.0 (10 mM phosphate buffer).

Discussion

Stacked structure of the heteroclusters: Our heterodimer design is based on the pseudo “base-pairing” of threoninol nucleotides incorporated at the center of an ODN. In contrast with natural A–T and/or G–C base-pairs, however, paired threoninol nucleotides stack with each other through hydrophobic stacking interactions. Therefore there are two possible stacked structures in which dyes are located either adjacent to the 5'-side (**M/Z**) or the 3'-side (**Z/M**) of the natural nucleobase (see Scheme 1). NMR analyses of an NMR-**Ma**/NMR-**Zb** duplex clearly revealed that the dyes were located adjacent to the 5'-side (**M/Z**), and other minor structures were rarely observed. This stacked structure can be explained by the space between the threoninol and natural nucleotide, in which a dye at the counterstrand is inserted. As shown in Figure 11, the number of atoms from the dye to a rigid five-membered ring is five between the crotches of ribose and threoninol at the 3'-side, whereas it is four at the 5'-side. Thus, the 3'-side is one carbon longer than the 5'-side, due to the 5'-carbon of the natural ribose scaffold,

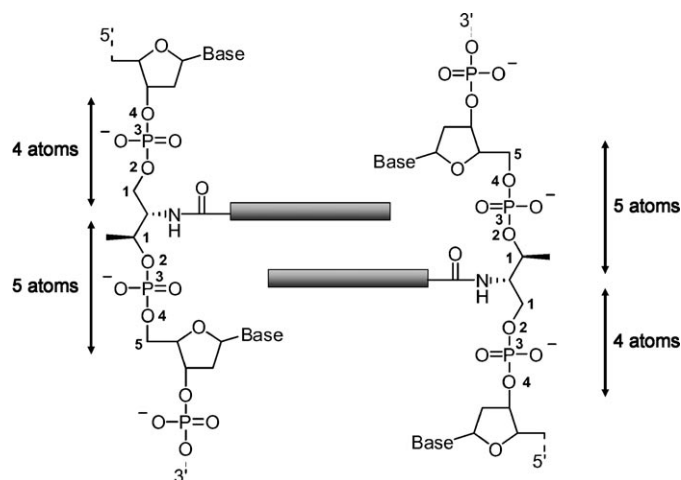


Figure 11. Illustration of the stacking manner of the dyes from each strand. The number of atoms from the dye to the rigid five-membered ring is five between the crotches of ribose and threoninol at the 3'-side, whereas it is four at the 5'-side. The number labeled in the figure indicates the atoms between the crotches of ribose and threoninol.

which facilitates the intercalation of the dye from the counterstrand. Computer modeling also supported the 5'-side **M/Z** orientation of the dye in the ODN dimer. In this model, both dyes from each strand fitted well into the space at the 5'-side of each other and were stacked in an antiparallel manner. Furthermore, stacked dyes of the unwound structure, shown in Figure 4b, are also consistent with the small ICDs measured (Figure 10). As reported previously, dyes conjugated to threoninols do not need winding in order to form a firmly stacked structure, and the flexibility of this structure allows the formation of a ladder-like structure.^[9b] It is also expected that a heterocluster of two different dyes, such as **Z3a/M3b**, **H3a/M3b**, **R3a/M3b**, or **N3a/M3b**, would be alternately aligned in the same manner as the 5'-side **M/Z** orientation (Figure 2 in Supporting Information).

Comparison of the spectroscopic behavior of the heterodimer with the molecular exciton model: As shown in Figures 6 to 8, all four heterodimers exhibited UV/Vis spectra that were distinctly different from those calculated from the sum-spectrum, and this difference depended on the $\Delta\lambda_{\max}$ of the combined dyes. Next is an explanation of these spectroscopic behaviors by the molecular exciton theory.^[1,4a,5b,6,7]

Spectral behavior predicted from the molecular exciton theory: Figure 12 shows a schematic illustration of the energy diagram of two laterally stacked dyes of different λ_{\max} . When monomer A of a higher transition energy is excitonically coupled with a dye of lower transition energy, the excited state splits into two energy levels.^[5b,7,17] The higher energy level corresponds to the in-phase transition in which the transition dipole moments of the monomers A and B have the same direction. In this case, the energy level becomes higher than that of monomer A due to the repulsive interaction between the two transition dipoles. The absorp-

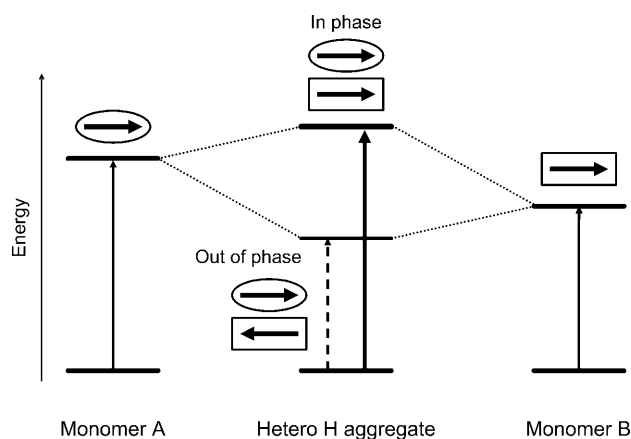


Figure 12. Schematic energy diagram of the heterodimer depicted on the basis of the exciton model. Each arrow, outlined by an ellipse or an oblong, designates the transition dipole moment.

tion coefficient of the in-phase transition is expected to increase due to the sum of the transitions A and B. In contrast, the energy level of the out-of-phase transition becomes lower than that of monomer B, due to the attractive interaction. However, the absorption coefficient of this transition decreases because the transition moment is partially cancelled due to its antiparallel orientation. The above excitonic interaction (namely, coherency) should be enhanced when the gap between the transition energies of monomers A and B, $\Delta\lambda_{\max}$, decreases. In the case where the transition moment of A is the same as that of B (i.e., A and B are the same dye), an out-of-phase transition is forbidden due to the complete cancellation of transition moment, whereas the in-phase transition is maximized.^[18]

Comparison with experimental results: The experimental results almost completely coincide with the above predictions based on the molecular exciton theory, with the exception of the results obtained for the spectral shift. In the case of **Z1a/M1b**, the band of the shorter wavelength (higher transition energy), derived from the azobenzene transition, displayed hyperchromism, whereas that of the longer wavelength (lower transition energy), derived from Methyl Red, displayed hypochromism. Both hyper- and hypochromism were enhanced in the **H1a** and **M1b** combination, because the $\Delta\lambda_{\max}$ of this combination was smaller than that between **Z1a** and **M1b**. These absorbance changes qualitatively coincided with the prediction based on the molecular exciton theory. In the case of **R1a/M1b** and **N1a/M1b**, which displayed a much smaller $\Delta\lambda_{\max}$, the out-of-phase transition became much weaker and hence a single sharp band, corresponding to an enhanced in-phase transition, appeared. The broad, weak shoulder observed at the longer wavelength may correspond to a weakened, out-of-phase transition. Thus, the molecular exciton theory of heterodimer formation was qualitatively validated from the viewpoint of transition intensity.

However, the spectral shift corresponding to the in-phase transition that we observed did not fit with the theory. According to the theory, an in-phase transition (higher transition energy) induces a hypsochromic shift with respect to the transition of monomer A, whereas an out-of-phase transition (lower transition energy) induces a bathochromic shift with respect to the transition of monomer B. Our experimental results revealed that the out-of-phase transition displayed a bathochromic shift (**Z1a/M1b** and **H1a/M1b**, Figures 6 and 7), in accordance with the theory. However, the in-phase transition also showed a bathochromic shift, which is contrary to the theory. Other combinations that were examined, such as **R1a/H1b** and **Z1a/H1b**, also exhibited bathochromicity of the in-phase transition (Figure 3 in Supporting Information). In order to rule out the possibility that this bathochromicity was induced simply by intercalation with the base-pairs of the ODN,^[19] we analyzed the hybridization of **H1a** with a natural **C** strand, which does not contain any threoninol nucleotides. Our previous NMR investigations demonstrated that such a sequence design (**H1a/C** duplex) facilitates intercalation of the dye tethered to threoninol between the base pairs.^[20] As shown in Figure 13,

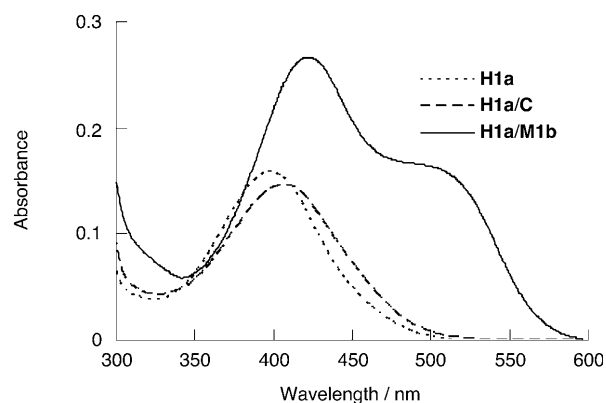


Figure 13. UV/Vis spectra of the **H1a/M1b** duplex (solid line), the **H1a/C** duplex (dashed line) and the single-stranded **H1a** (dotted line) at 0°C. Solution conditions were as follows: [ODN] = 5 μM , [NaCl] = 100 mM, pH 7.0 (10 mM phosphate buffer).

single-stranded **H1a**, double-stranded **H1a/C**, and double-stranded **H1a/M1b** had λ_{\max} at 398, 408, and 422 nm, respectively. The bathochromicity induced by hybridization of **H1a** with **C** was only 10 nm (compare the dotted and dashed lines in Figure 13), indicating that the presence of the adjacent bases did not much affect the spectral shift. However, **H1a/M1b** allowed a bathochromic shift as large as 24 nm (compare the solid and dotted lines in Figure 13), which was obviously larger than that induced by the **H1a/C** duplex.^[21] Hence, we conclude that the bathochromicity of the in-phase transition cannot be explained by the conventional molecular exciton theory.

Since the conventional molecular exciton theory is based on the point-dipole approximation model, this may cause problems in its application to a firmly stacked heterodimer,

because stacked dyes of 10 Å size that are in close proximity (3.5 Å) cannot be approximated as a “point”.^[1] A further improved model (such as the extended dipole approximation^[1] and/or molecular transition density^[22]) will be needed to explain the bathochromic shift of heterodimerization. At present, we think that this discord may be due to the orbital overlap between two dyes firmly stacked close to each other in a duplex. Currently, quantum calculation (ab initio calculation) of the heterodimer is being applied to explain the bathochromic shift.

Heteroclustering of the dyes: As shown in Figure 9, an increase in the dye number resulted in intensification of the in-phase transition together with a hypsochromic shift, whereas the corresponding out-of-phase transition did not. This spectroscopic behavior is very similar to that of homo H-aggregates in which identical dyes are axially stacked. Although the hypsochromic shift was smaller than that seen for homo H-aggregates, these results clearly demonstrate that strong coherent coupling occurred even among the heteroclusters. Even **H3a/M3b**, which had a $\Delta\lambda_{\max}$ of 82 nm, exhibited almost a single band due to the strong coherent coupling within the heterocluster. We can predict from this result that one- or two-dimensional clusters, composed of two different dyes with different absorption maxima, should exhibit essentially a single band when the dyes are assembled in an orderly fashion, and should show strong coherency (exciton coupling).^[4]

Conclusions

The NMR study revealed that different dyes incorporated at the center of an ODN through tethering to D-threoninols were stacked antiparallel to each other, and were located adjacent to the 5'-side of a natural nucleobase.

Heterodimerization induced hyperchromism of the band of the shorter wavelength (in-phase transition), but hypochromism of the band of the longer wavelength, and these absorbance changes were enhanced when the $\Delta\lambda_{\max}$ of the two dyes was decreased. Furthermore, both bands exhibited a distinct bathochromic shift. These spectroscopic behaviors were consistent with the shifts predicted from the molecular exciton theory, except for the bathochromic shift of the in-phase transition. This discordance might be due to limitations of the point dipole approximation of the conventional molecular exciton theory.

An increase in dye number dramatically intensified the in-phase transition, which resulted in the spectrum of the heterocluster being almost a single absorption band even though the two dyes had different absorption maxima.

Thus, we have presented, for the first time, a qualitative comparison of the actual spectroscopic behavior of heterodimers with the spectroscopic behavior predicted for such heterodimers by the molecular exciton theory, by systematically changing the $\Delta\lambda_{\max}$ of the two dyes. We are now conducting a quantitative comparison of the present experimen-

tal results with theoretical predictions based on ab initio calculations.

Our results partly explain the spectroscopic behavior of intercalation. In general, dyes show batho- and hypochromicity when they are intercalated between the base pairs of a duplex. According to Sarkar et al., this bathochromic shift is due to the change in local polarity around the chromophore.^[19] However, we demonstrate here that exciton coupling of a natural nucleobase ($\lambda_{\max} \approx 260$ nm) with an intercalated dye (λ_{\max} should be longer than 260 nm) also partly contributes to the weak but distinct bathochromic shift and hypochromicity. Furthermore, the design of a fluorophore and a quencher pair, tethered to D-threoninols, with a smaller $\Delta\lambda_{\max}$ should result in a highly sensitive molecular beacon based on a firmly stacked fluorophore–quencher heterodimer with greater coherency. The molecular design of a new heterodimer of a fluorophore–quencher pair as a component of a molecular beacon is currently underway.

Experimental Section

Materials: All the conventional phosphoramidite monomers, CPG columns, reagents for DNA synthesis, and Poly-Pak II cartridges were purchased from Glen Research. Other reagents for the synthesis of the phosphoramidite monomer were purchased from Tokyo Kasei Co. and Sigma-Aldrich.

Synthesis of DNA modified with H, M, N, R, or Z: All the modified DNAs were synthesized by using an automated DNA synthesizer (ABI-3400 DNA synthesizer, Applied Biosystems) with conventional and dye-carrying phosphoramidite monomers. Azobenzene, Methyl Red, and Naphthyl Red phosphoramidite monomers were synthesized according to a previous report.^[19b,23] The compounds 4'-methylthioazobenzene and 4'-dimethylamino-2-nitroazobenzene, synthesized according to the literature,^[24,25] were converted to phosphoramidite monomers as described in Scheme 1 of the Supporting Information. The coupling efficiency of the monomers with modified residues was as high as that of the conventional monomers, as judged from the intensity of the color of the released trityl cation. After the recommended workup, the oligomers were purified by reverse-phase HPLC and characterized by MALDI-TOFMS (Autoflex II, Bruker Daltonics).

The MALDI-TOFMS data, observed (found) versus calculated (calcd.), for the monomers were: **Z1a**: calcd for [**Z1a**+H]⁺: 4020; found: 4020; **Z2a**: calcd for [**Z2a**+H]⁺: 4395; found: 4395; **Z3a**: calcd for [**Z3a**+H]⁺: 4770; found: 4770; **H1a**: calcd for [**H1a**+H]⁺: 4066; found: 4067; **H2a**: calcd for [**H2a**+H]⁺: 4487; found: 4488; **H3a**: calcd for [**H3a**+H]⁺: 4908; found: 4909; **R1a**: calcd for [**R1a**+H]⁺: 4108; found: 4108; **R2a**: calcd for [**R2a**+H]⁺: 4571; found: 4572; **R3a**: calcd for [**R3a**+H]⁺: 5034; found: 5035; **N1a**: calcd for [**N1a**+H]⁺: 4113; found: 4113; **N2a**: calcd for [**N2a**+H]⁺: 4581; found: 4581; **N3a**: calcd for [**N3a**+H]⁺: 5049; found: 5050; **M1b**: calcd for [**M1b**+H]⁺: 4063; found: 4065; **M2b**: calcd for [**M2b**+H]⁺: 4481; found: 4481; **M3b**: calcd for [**M3b**+H]⁺: 4899; found: 4899; NMR-**Ma**: calcd for [MMR-**Ma**+H]⁺: 2211; found: 2211; NMR-**Zb**: calcd for [MMR-**Zb**+H]⁺: 2167; found: 2168.

Spectroscopic measurements: The UV/Vis and CD spectra were measured on a JASCO model V-550 spectrophotometer and a JASCO model J-820 spectropolarimeter, respectively, with a 10 mm quartz cell. Both models were equipped with programmable temperature controllers. The conditions of the sample solutions were as follows (unless otherwise noted): [NaCl]=100 mM, pH 7.0 (10 mM phosphate buffer), [DNA]=5 μ M. For measurements at pH 5.0, 10 mM MES buffer was used. All samples of DNA–dye conjugates were heated at 80 °C for 5 min in the dark, to thermally isomerize the *cis* form, which might be photoisomerized by the ambient light, to *trans* form before spectroscopic measurement.^[26]

Measurement of melting temperature: The melting curve of duplex DNA was obtained by measurement of the change in absorbance at 260 nm versus temperature (unless otherwise noted), using a spectrophotometer as described above. The melting temperature (T_m) was determined from the maximum of the first derivative of the melting curve. Both the heating and the cooling curves were measured, and the obtained T_m values agreed to within 2.0°C. The temperature ramp was 1.0°C min⁻¹. The conditions of the sample solutions were the same as those described for the above spectroscopic measurements.

NMR measurements: NMR samples were prepared by dissolving three-times-lyophilized DNA (modified and complementary DNA) in a H₂O/D₂O 9:1 containing 20 mM sodium phosphate (pH 7.0), to give a duplex concentration of 1.0 mM. NaCl was added to give a final sodium concentration of 200 mM. NMR spectra were measured with a Varian INOVA spectrometer (700 MHz) equipped for triple resonance at a probe temperature of 278 K. Resonances were assigned by standard methods using a combination of 1D, TOCSY (60 ms of mixing time), DQF-COSY, and NOESY (150 ms of mixing time) experiments. All spectra in the H₂O/D₂O 9:1 were recorded using the 3–9–19 WATERGATE pulse sequence for water suppression.

Computer modeling: Molecular modeling by conformational energy minimization was performed with the InsightII/discover3 software (Molecular Simulation, Inc.) on a Silicon Graphics O2+ workstation with the operating system IRIX64 Release 6.5, and the AMBER force field was used for the calculations. The results of the NMR analyses served as a starting point for the modeling. For the analysis, a dimer of Methyl Red and azobenzene was prepared by positioning the two dye molecules in a cofacial orientation and replacing two native base pairs.

Acknowledgements

This work was supported by the Core Research for Evolution Science and Technology (CREST) and Japan Science and Technology Agency (JST). Partial support was provided by a Grant-in-Aid for Scientific Research from the Ministry of Education, Culture, Sports, Science and Technology, Japan and also the Mitsubishi Foundation (for H.A.). We thank Dr. Kyoichi Sawabe (Department of Molecular Design and Engineering, Nagoya University) for his helpful discussions on the molecular exciton theory.

- [1] T. Kobayashi, *J-aggregates*, World Scientific, Singapore, **1996**, pp. 1–40.
- [2] a) W. Lin, W. Lin, G. K. Wong, T. J. Marks, *J. Am. Chem. Soc.* **1996**, *118*, 8034–8042; b) O. R. Evans, W. Lin, *Acc. Chem. Res.* **2002**, *35*, 511–522; c) E. L. Botvinick, J. V. Shah, *Methods Cell Biol.* **2007**, *82*, 81–109.
- [3] a) S. Bahatyrova, R. N. Freses, C. A. Siebert, J. D. Olsen, K. Van Der Werf, R. Van Grondelle, R. A. Niederman, P. A. Bullough, C. Otto, C. N. Hunter, *Nature* **2004**, *430*, 1058–1062; b) T. S. Balaban, N. Berova, C. M. Drain, R. Hauschild, X. Huang, H. Kalt, S. Lebedkin, J.-M. Lehn, F. Nifaitis, G. Pescitelli, V. I. Prokhorenko, G. Riedel, G. Smeureanu, J. Zeller, *Chem. Eur. J.* **2007**, *13*, 8411–8427; c) J. D. Olsen, J. D. Tucker, J. A. Timney, P. Qian, C. Vassilev, C. N. Hunter, *J. Biol. Chem.* **2008**, *283*, 30772–30779.
- [4] a) M. Kasha, *Radiat. Res.* **1963**, *20*, 55–71; b) J. L. Seifert, R. E. Connor, S. A. Kushon, B. A. Armitage, *J. Am. Chem. Soc.* **1999**, *121*, 2987–2995; c) M. Wang, G. L. Silva, B. A. Armitage, *J. Am. Chem. Soc.* **2000**, *122*, 9977–9986; d) N. R. Conley, A. K. Pomerantz, H. Wang, R. J. Twieg, W. E. Moerner, *J. Phys. Chem. B* **2007**, *111*, 7929–7931; e) S. Ikeda, A. Okamoto, *Chem. Asian J.* **2008**, *3*, 958–968.
- [5] a) K. Murata, S. Kuroda, K. Saito, *Thin Solid Films* **1997**, *295*, 73–76; b) B. Z. Packard, D. D. Topygin, A. Koriya, L. Brand, *J. Phys. Chem. B* **1998**, *102*, 752–758; c) R. A. Garoff, E. A. Litzinger, R. E. Connor, I. Fishman, B. A. Armitage, *Langmuir* **2002**, *18*, 6330–6337; d) A. Yamaguchi, N. Kometani, Y. Yonezawa, *Thin Solid Films* **2006**, *513*, 125–135; e) H. Bittermann, D. Siegemund, V. L. Malinovskii, R. Häner, *J. Am. Chem. Soc.* **2008**, *130*, 15285–15287; f) I. V. Astakhova, V. A. Kurshun, J. Wengel, *Chem. Eur. J.* **2008**, *14*, 11010–11026; g) Y. N. Teo, J. N. Wilson, E. T. Kool, *J. Am. Chem. Soc.* **2009**, *131*, 3923–3933.
- [6] V. Czikkely, G. Dreizler, H. D. Försterling, H. Kuhn, J. Sondermann, P. Tillmann, J. Z. Wiegand, *Naturforsch.* **1969**, *24a*, 1821–1830.
- [7] a) S. Bernacchi, Y. Mély, *Nucleic Acids Res.* **2001**, *29*, e62; b) S. Bernacchi, E. Piémont, N. Potier, A. V. Dorsselaer, Y. Mély, *Biophys. J.* **2003**, *84*, 643–654.
- [8] a) S. Tyagi, F. R. Kramer, *Nat. Biotechnol.* **1996**, *14*, 303–308; b) M. K. Johansson, H. Fidder, D. Dick, R. M. Cook, *J. Am. Chem. Soc.* **2002**, *124*, 6950–6956; c) E. Socher, L. Bethge, A. Knoll, N. Jungnick, A. Herrmann, O. Seitz, *Angew. Chem.* **2008**, *120*, 9697–9701; *Angew. Chem. Int. Ed.* **2008**, *47*, 9555–9559.
- [9] a) H. Kashida, H. Asanuma, M. Komiyama, *Angew. Chem.* **2004**, *116*, 6684–6687; *Angew. Chem. Int. Ed.* **2004**, *43*, 6522–6525; b) H. Kashida, T. Fujii, H. Asanuma, *Org. Biomol. Chem.* **2008**, *6*, 2892–2899.
- [10] There are two possible structures for the heterodimer, as shown in Scheme 1.
- [11] a) C. Brotschi, C. J. Leumann, *Angew. Chem.* **2003**, *115*, 1694–1697; *Angew. Chem. Int. Ed.* **2003**, *42*, 1655–1658; b) C. Brotschi, G. Mathis, C. J. Leumann, *Chem. Eur. J.* **2005**, *11*, 1911–1923; c) Z. Johar, A. Zahn, C. J. Leumann, B. Jaun, *Chem. Eur. J.* **2008**, *14*, 1080–1086; d) A. Zahn, C. J. Leumann, *Chem. Eur. J.* **2008**, *14*, 1087–1094.
- [12] The melting temperature was measured in the presence of 100 mM NaCl at pH 7.0 (10 mM phosphate buffer). The concentration of NMR-Ma/NMR-Zb was 5 μM. The melting temperature of the duplex under NMR measurement conditions should be much higher because the concentrations of both NaCl and modified ODNs are higher: a) R. Owczarzy, Y. You, B. G. Moreira, J. A. Manthey, L. Huang, M. A. Behlke, J. A. Walder, *Biochemistry* **2004**, *43*, 3537–3554; b) H. Long, A. Kudlay, G. C. Schatz, *J. Phys. Chem. B* **2006**, *110*, 2918–2926.
- [13] M. Liu, X. Mao, C. Ye, J. K. Nicholson, J. C. Lindon, *J. Magn. Reson.* **1998**, *132*, 125–129.
- [14] a) E. Sawicki, *J. Org. Chem.* **1957**, *22*, 915–919; b) R. K. Burkhard, R. D. Bauer, D. H. Klaassen, *Biochemistry* **1962**, *1*, 819–827; c) T. Sueyoshi, N. Nishimura, S. Yamamoto, S. Hasegawa, *Chem. Lett.* **1974**, 1131–1134; d) P. C. Chen, Y. C. Chieh, J. C. Wu, *J. Mol. Struct.* **2005**, *733-779*, 183–189.
- [15] Since the absorption spectra also slightly depended on the temperature being higher than the T_m at which the duplex was dissociated into two single-strands, chromophore motion also affected the ground-state spectra slightly.
- [16] A. H. Herz, *Photogr. Sci. Eng.* **1974**, *18*, 323.
- [17] N. Berova, K. Nakanishi, *Circular Dichroism. Principles and Applications*, (Eds: N. Berova, K. Nakanishi, R. W. Woody), Wiley-VCH, New York, **2000**, pp. 340–344.
- [18] This is what we call the H-band, which displays distinct hypsochromicity.
- [19] D. Sarkar, P. Das, S. Basak, N. Chattopadhyay, *J. Phys. Chem. B* **2008**, *112*, 9243–9249.
- [20] X. G. Liang, H. Asanuma, H. Kashida, A. Takasu, T. Sakamoto, G. Kawai, M. Komiyama, *J. Am. Chem. Soc.* **2003**, *125*, 16408–16415.
- [21] Since exciton splitting depended on the $\Delta\lambda_{\max}$ between these dyes and DNA, the effect of natural base on the chromophore–chromophore splitting might be small. Furthermore, since the dye has already been located next to the natural base in the single strand, the adjacent natural base did not greatly affect the spectral change (exciton coupling) of incorporated dyes by hybridization.
- [22] K. Norland, A. Ames, T. Taylor, *Photogr. Sci. Eng.* **1970**, *14*, 295–307.
- [23] a) H. Asanuma, H. Kashida, X. G. Liang, M. Komiyama, *Chem. Commun.* **2003**, 1536–1537; b) H. Asanuma, K. Shirasuka, T. Takar-

- ada, H. Kashida, M. Komiyama, *J. Am. Chem. Soc.* **2003**, *125*, 2217–2223.
- [24] a) W. H. Nutting, R. A. Jewell, H. Rapoport, *J. Org. Chem.* **1970**, *35*, 505–508; b) M. A. Rahim, P. N. P. Rao, E. E. Knaus, *J. Heterocycl. Chem.* **2002**, *39*, 1309–1314.
- [25] K. A. Bello, *Dyes Pigm.* **1989**, *11*, 65–76.
- [26] H. Nishioka, X. Liang, H. Kashida, H. Asanuma, *Chem. Commun.* **2007**, 4354–4356.

Received: April 10, 2009
Published online: August 31, 2009